

**NASA  
Technical  
Paper  
2146**

**AUGUST 1983**

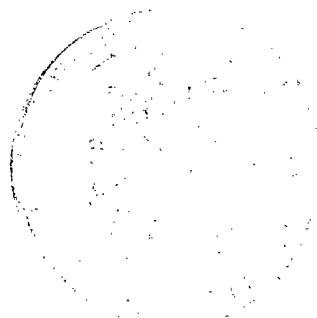
NASA  
TP  
2146  
c.1



# **Cavitation Pitting and Erosion of Aluminum 6061-T6 in Mineral Oil and Water**

**Bezzam C. S. Rao and  
Donald H. Buckley**

**LOAN COPY. RETURN TO  
AFWL TECH LIBRARY  
KIRTLAND AFB, N.M. 87117**



25th Anniversary  
1958-1983

**NASA  
Technical  
Paper  
2146**

**1983**

TECH LIBRARY KAFB, NM



0134983

# **Cavitation Pitting and Erosion of Aluminum 6061-T6 in Mineral Oil and Water**

**Bezzam C. S. Rao and  
Donald H. Buckley**  
*Lewis Research Center  
Cleveland, Ohio*

**NASA**

National Aeronautics  
and Space Administration

Scientific and Technical  
Information Branch

## Summary

Cavitation erosion studies on aluminum 6061-T6 in mineral oil and in ordinary tap water are presented. The maximum erosion rate (MDPR, or mean depth of penetration rate) in mineral oil was about four times that in water. The MDPR in mineral oil decreased continuously with time, but the MDPR in water remained approximately constant. The cavitation pits in mineral oil were of smaller diameter and depth than the pits in water. Treating the pits as spherical segments, we computed the radius  $r$  of the sphere. The logarithm of  $h/a$ , where  $h$  is the pit depth and  $2a$  is the top width of the pit, was linear when plotted against the logarithm of  $2r/h - 1$ .

## Symbols

- $a$  pit radius at surface
- $h$  pit depth
- $P(R)$  pressure at bubble wall
- $P_i(R)$  total vapor and gas pressure in bubble
- $P_0$  ambient pressure in liquid
- $P_v$  vapor pressure of liquid
- $R$  bubble radius
- $r$  radius of cavitation pit
- $t$  time
- $U$  bubble wall collapse velocity,  $dR/dt$
- $\sigma$  surface tension of liquid
- $\mu$  viscosity of liquid

## Introduction

Cavitation erosion in engine bearings has been of increasing importance in the past decade, perhaps because of the design trends toward higher rotational speeds. This phenomenon is predominantly observed in diesel engine bearings and on rare occasions in gasoline engines operated under sustained overspeed or with incorrect ignition timing (ref. 1). Many examples of cavitation erosion in bearings are reported by Wilson (ref. 2), Summers-Smith (ref. 3), Conway-Jones (ref. 4), and James (ref. 5). A brief review of cavitation in bearings was recently published by Dowson and Taylor (ref. 6).

Hunt et al. (ref. 7) report a study concerning the occurrence of cavitation between meshing gear teeth in an oil-lubricated gearbox. Heathcock and Protheroe (ref. 8) report the possible occurrence of cavitation in gold-mining machines operated with water-base fluids, typically 5-percent-oil-in-water emulsions.

In spite of the increasing importance of cavitation erosion of different materials in oils, not many studies on

this topic have been reported in the literature. Endo et al. (ref. 9) report cavitation erosion studies of 0.09 percent carbon steel in spindle oil and of tin-base white metal in spindle oil, in machine oil, and in silicon oil. Garner et al. (ref. 1) studied the erosion resistance of some tin-, copper-, and lead-base bearing materials in Shell Rotella 30 oil. Soda and Tanaka (ref. 10) report the cavitation erosion patterns and the pressure distributions over the test specimen surface in SAE 20 oil.

The authors are presently studying the cavitation erosion of different bearing metals and alloys in mineral oils. This report presents the variations of weight loss, the surface roughness, and the pit diameter and depth caused by cavitation erosion on aluminum 6061-T6 in mineral oil D21 and water.

## Experimental Equipment and Test Conditions

The experiments were carried out in an ultrasonic magnetostrictive oscillator operating at 20-kHz frequency and 50- $\mu$ m double amplitude. The material for the test specimens was commercially pure aluminum 6061-T6 rod, 12.7 mm in diameter. The mechanical properties of aluminum 6061-T6 are presented in table I. The test liquids were mineral oil D21 and ordinary tap water, whose physical properties are given in table II.

TABLE I. - MECHANICAL PROPERTIES OF ALUMINUM 6061-T6

Density, kg/m <sup>3</sup> .....	2700
Yield strength, MN/m <sup>2</sup> .....	110
Ultimate tensile strength, MN/m <sup>2</sup> .....	276
Elastic modulus, MN/m <sup>2</sup> .....	71 $\times$ 10 <sup>3</sup>
Ultimate resilience, MN/m <sup>2</sup> .....	0.54
Elongation, percent .....	12
Hardness, Bhn .....	95
Nominal composition .....	0.6 Si, 0.25 Cu, 1.0 Mg, 0.25 Zn

TABLE II. - PHYSICAL PROPERTIES OF MINERAL OIL D21 AND WATER

Property	Mineral oil D21	Water
Density, kg/m <sup>3</sup>	869	1000
Kinematic viscosity at 20° C, cS	110	1.01
Surface tension at 20° C, dynes/cm	33.2	73.6
Bulk modulus, MPa	1.7 $\times$ 10 <sup>3</sup>	2.18 $\times$ 10 <sup>2</sup>
Flashpoint, °C	213	-----
Pour point, °C	-9.4	-----

The test specimen was subjected to cavitation, and weight loss measurements were taken at 5-min intervals for the tests in mineral oil and at 5-min intervals for the first 35 min and then at 15-min intervals in water.

## Experimental Results and Discussion

### Weight Loss

The variations of cumulative weight loss of the test specimen in mineral oil and in ordinary tap water are presented in figure 1. The corresponding mean depth of penetration rates (MDPR) in the two liquids are presented in figure 2. As figure 1 shows, aluminum 6061-T6 eroded much faster in mineral oil than in water

initially, without showing any incubation period. However, as the test time increased, the rate of weight loss (or MDPR) in mineral oil decreased continuously, but the MDPR in water remained approximately constant. This was apparently caused by the rapid attenuation of pressure waves in mineral oil as the depth of erosion increased. The peak MDPR in mineral oil was four times that in water. The eroded surfaces at test times of 40 min in mineral oil and 90 min in water are shown in figure 3.

### Surface Topography

Surface profiles of aluminum 6061-T6 tested in mineral oil for 4, 20, and 40 min are shown in figure 4. A

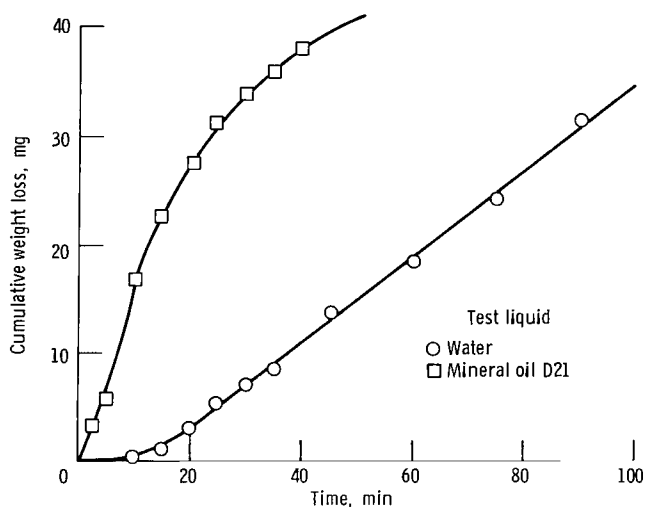


Figure 1. - Cumulative weight loss of aluminum 6061-T6 as a function of test time.

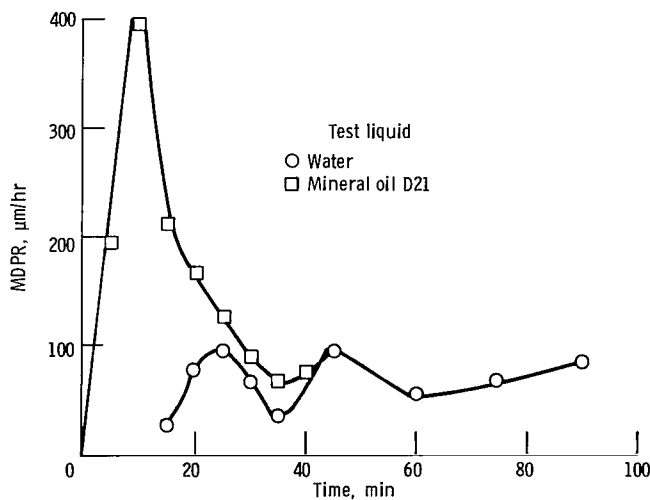
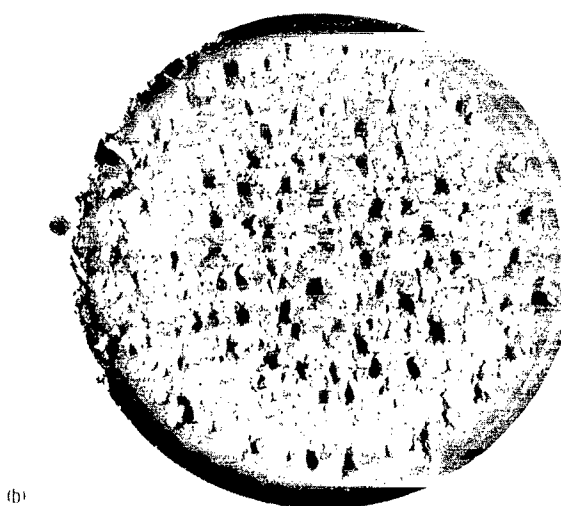
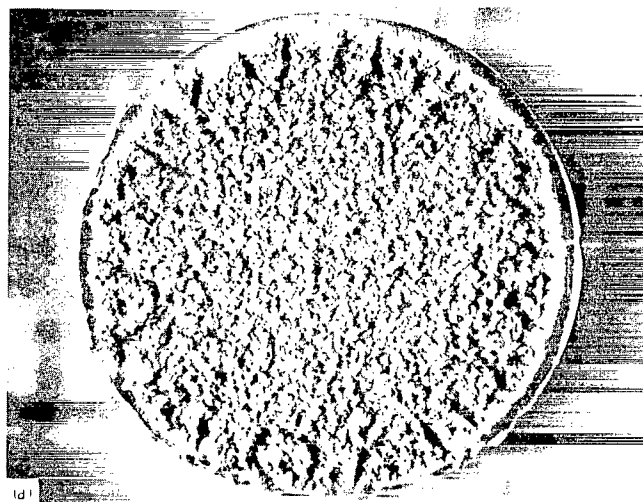


Figure 2. - Mean depth of penetration rate (MDPR) for aluminum 6061-T6 as a function of test time.



(a) After testing for 40 min in mineral oil D21.  
(b) After testing for 90 min in water.

Figure 3. - Eroded surfaces of aluminum 6061-T6.

number of pits of varying depths selected from the profiles are plotted one below the other in figure 5. The pit depth shown in this figure varies from about 7.5 to 125  $\mu\text{m}$ , and the top width (diameter) varies from about 55 to 450  $\mu\text{m}$ .

Surface profiles of aluminum 6061-T6 tested in water for 20, 60, and 90 min are shown in figure 6. A selected number of pits are plotted one below the other in figure 7. The pit depth shown in this figure varies from about 7.5 to 240  $\mu\text{m}$ , and the top width (diameter) varies from about 55 to 950  $\mu\text{m}$ . A study of figures 4 to 7 together with figure 3 indicates that erosion in mineral oil is more uniformly distributed over the specimen surface than erosion in water. For the same erosion time, the erosion pits in water are about two times deeper than those in mineral oil, but fewer in number. The computed mean depth of penetration (MDP) for the specimen tested in water for 90 min was 93  $\mu\text{m}$ , and the maximum pit depth measured was 250  $\mu\text{m}$ . The MDP for the specimen tested in mineral oil for 40 min was 110  $\mu\text{m}$ , and the maximum pit depth measured was 125  $\mu\text{m}$ .

The precise shape of the erosion pit is of importance in computing the energy absorbed by the material. To

obtain a physical appreciation of erosion pit shape, some selected pits were plotted to a natural scale (unlike the distorted scale of surface profiles in figs. 4 to 7). Figures 8 and 9 show these pits in mineral oil and in water, respectively.

### Discussion of Experimental Results

**Collapse times and pressures.** — The cavitation bubbles grow or collapse during one-quarter cycle of the oscillator, viz within 12.5  $\mu\text{sec}$ . Vyas and Preece (ref. 11) report that most bubbles in water collapse in about 5  $\mu\text{sec}$ . It is known that viscous effects alter the pressure at the bubble wall and thus reduce the effective pressure differential and consequently the rates of either bubble growth or collapse. The pressure  $P(R)$  at the bubble wall during collapse can be expressed (ref. 12) as

$$P(R) = P_i(R) - \frac{2\sigma}{R} + \frac{4\mu U}{R} \quad (1)$$

where

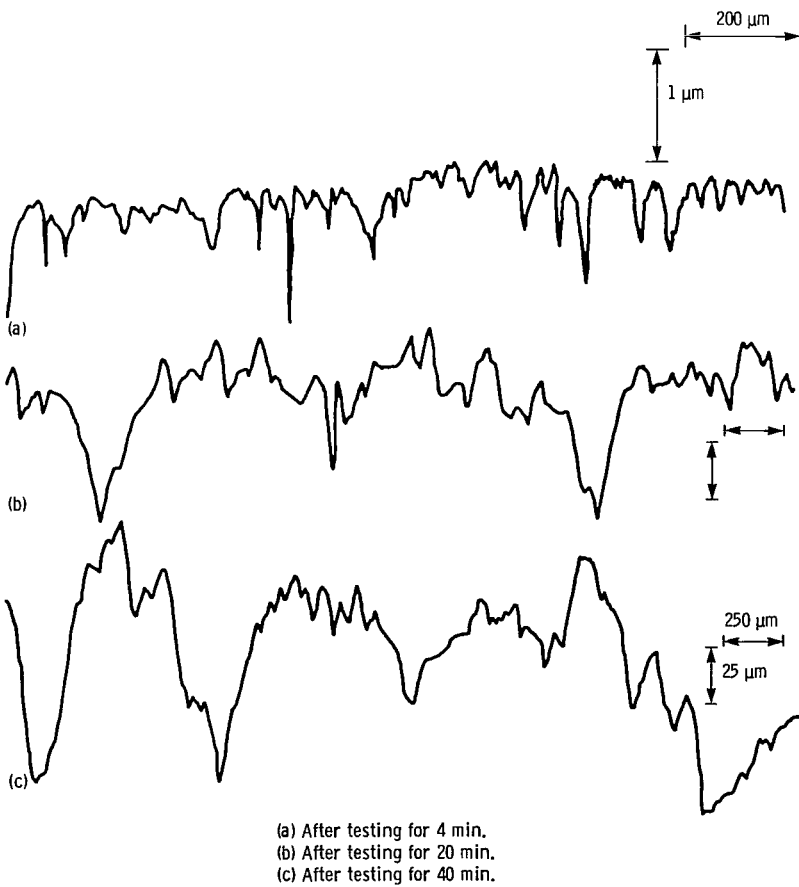


Figure 4. - Surface profiles of erosion on aluminum 6061-T6 tested in mineral oil D21.

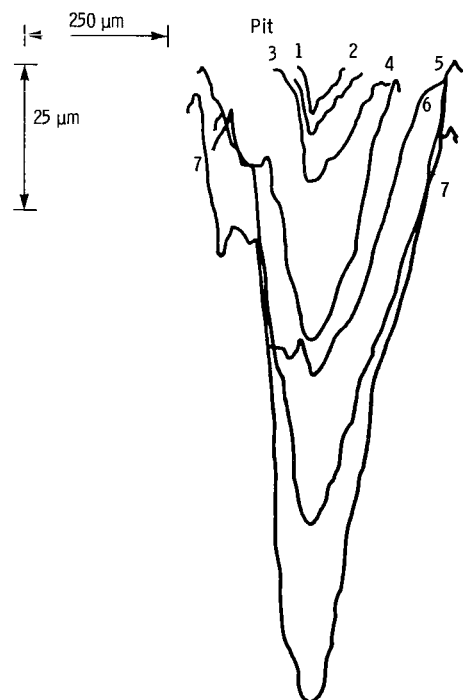
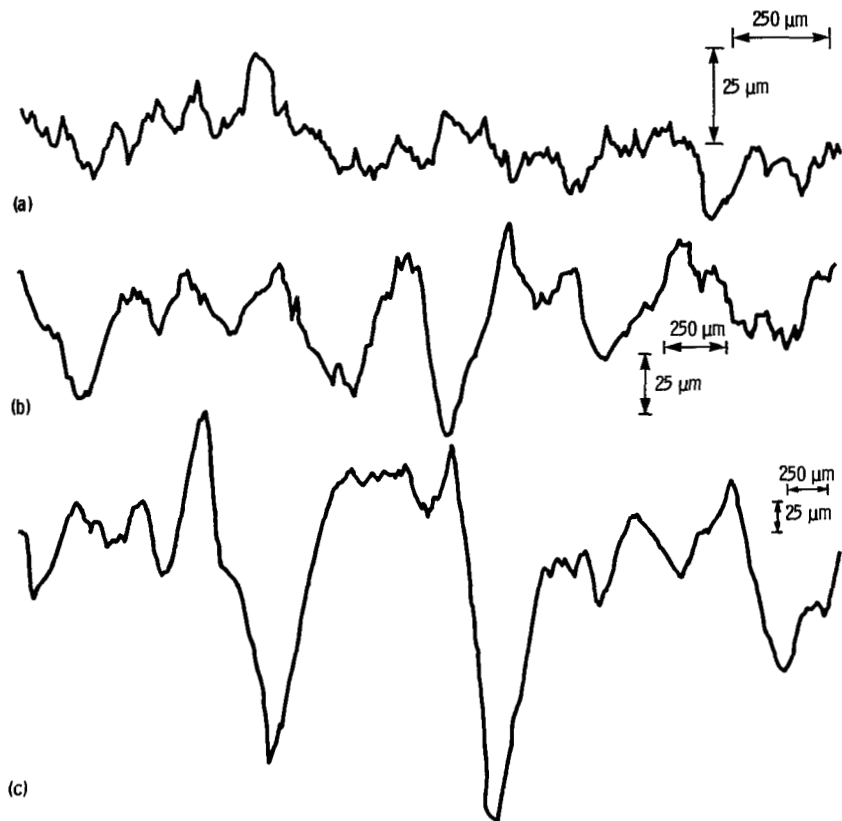


Figure 5. - Topography of selected erosion pits on aluminum 6061-T6 tested in mineral oil D21.



(a) After testing for 20 min.  
 (b) After testing for 60 min.  
 (c) After testing for 90 min.

Figure 6. - Surface profiles of erosion on aluminum 6061-T6 tested in water.

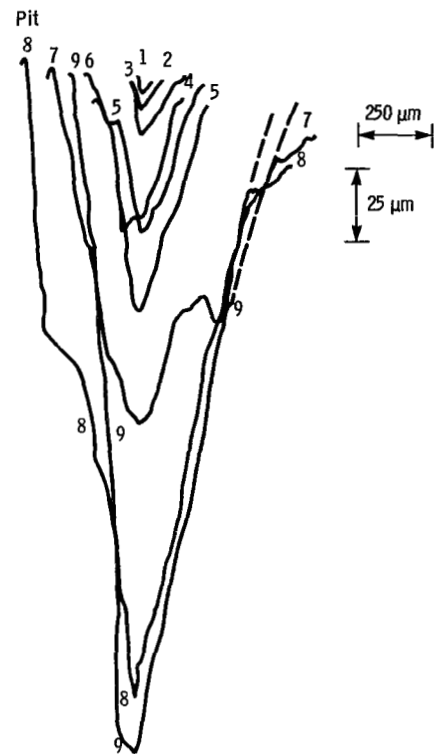


Figure 7. - Topography of selected pits of erosion on aluminum 6061-T6 tested in water.

- $P_i(R)$  total vapor and gas pressure in bubble
- $R$  bubble radius
- $\sigma$  surface tension of liquid
- $\mu$  viscosity of liquid
- $U$  bubble wall collapse velocity,  $dR/dt$
- $t$  time

The collapse pressures are generally computed (ref. 12) by assuming a bubble of initial radius  $R_0 = 1.27$  mm (50 mils). The pressure generated by the collapse of such a bubble to a size  $R/R_0 = 5 \times 10^{-3}$  is 95 245 MPa ( $9.4 \times 10^5$  atm). Vyas and Preece (ref. 11) measured a maximum stress amplitude of about 700 MPa ( $\sim 7 \times 10^3$  atm). If we assume the same size bubble in mineral oil also, the viscosity term in equation (1) has a negligible influence on the pressures generated. However, the erosion pits clearly show that the collapsing bubbles are smaller in mineral oil than in water. Also, the minimum radius  $R$  to which the bubbles collapse would be different in mineral oil than in water. If a bubble of initial radius  $R_0 = 2.54 \mu\text{m}$  (0.1 mil) collapses to a size  $R/R_0 = 1 \times 10^{-2}$ , the viscosity effect due to the third term on the right side of equation (1) could contribute as much as 75 percent of the total

pressure generated. The pressure generated by such a bubble works out to 253 MPa ( $2.5 \times 10^3$  atm). Plesset (ref. 13) computed that neglecting surface tension and viscous effects introduces a 1-percent error for bubbles of initial radius  $R_0 \geq 1$  mm collapsing under a pressure  $P_0 - p_v \geq 0.3$  MPa. The larger initial weight loss rate and the smaller pits in mineral oil observed in the present studies indicate that cavitation bubbles in mineral oil are smaller and have perhaps higher collapse pressures than cavitation bubbles in water.

**Nature of cavitation pits.** - A cavitation pit is generally assumed to be a segment of a sphere, as shown in figure 10. If  $2a$  is the chord diameter and  $h$  is the pit depth, the radius  $r$  of the sphere can be expressed as

$$r = \frac{a^2 + h^2}{2h} \quad (2)$$

Using equation (2), we computed the radii of the different pits and drew the spherical segments on the corresponding pits in figures 8 and 9. These figures show that the volume of the pits would be overestimated if it were calculated by treating them as spherical segments.

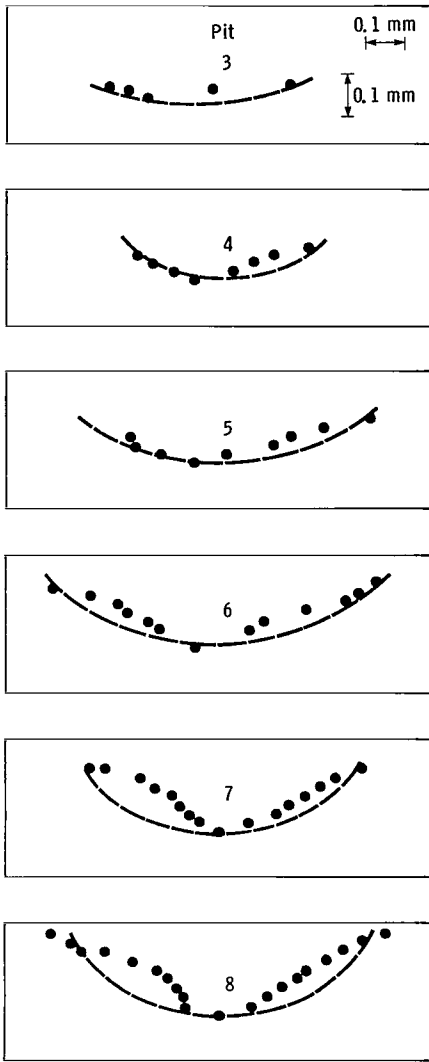


Figure 8. - Shape of pits on aluminum 6061-T6 tested in mineral oil D21.

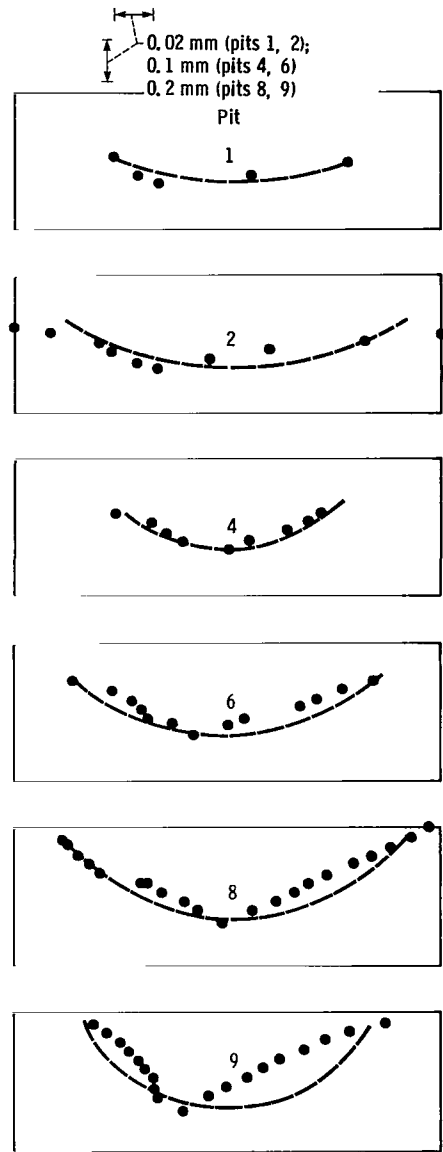


Figure 9. - Shape of pits on aluminum 6061-T6 tested in water.

The pits, in general, have a deep central portion with shallow, flat portions on either side.

Also, we can express

$$\frac{h}{a} = \frac{1}{\sqrt{2r/h - 1}} \quad (3)$$

or

$$\log \frac{h}{a} + \frac{1}{2} \log \left( \frac{2r}{h} - 1 \right) = 0 \quad (4)$$

Figure 11 shows the logarithm of  $h/a$  to be linear when plotted against the logarithm of  $2r/h - 1$ . The experimental points show a slope of  $-1/2$  because the

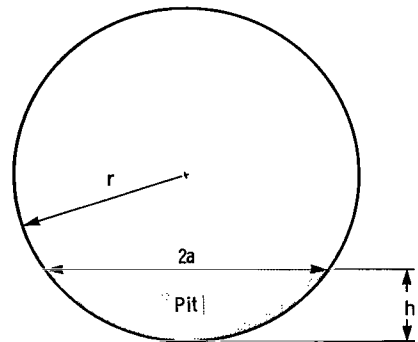


Figure 10. - Theoretical cavitation pit.

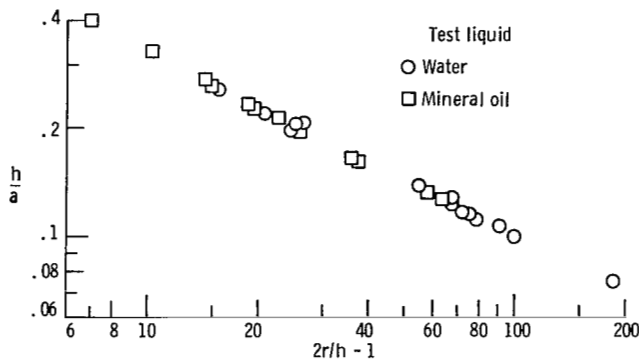


Figure 11. - Variation of ratio  $h/a$  with  $2r/h - 1$ , where  $h$  is pit depth,  $a$  is pit radius at surface, and  $r$  is radius of sphere.

value of  $r$  was computed from the values of  $h/a$ . The values of  $h/a$  are of significance in figure 11. In mineral oil, the  $h/a$  of individual pits varied from 0.125 to 0.400; in water, it varied from 0.075 to 0.260. In other words, for the same depth, the pits were wider in water than in mineral oil. This perhaps is due to the larger microjets striking the surface in water than in mineral oil indicating that cavitation bubbles grow to a larger size in water than in mineral oil.

Considering pits of depth less than  $15 \mu\text{m}$  only, we found that in mineral oil

$$\frac{h}{a} = 0.312 \quad (5)$$

and in water

$$\frac{h}{a} = 0.220 \quad (6)$$

Previous pit measurements of cavitation erosion in water by Robinson and Hammitt (ref. 14) indicated the ratio  $h/a$  to be 0.20. Stinebring et al. (ref. 15), using a microscope and collimated light beam, determined the minimum and maximum values of  $h/a$  to be 0.068 and 0.333, respectively, in water. This range of  $h/a$  values is in agreement with the present measurements. Equation (6) agrees closely with the measurements of Robinson and Hammitt.

## Summary of Results

Cavitation erosion studies on aluminum 6061-T6 in mineral oil D21 and water had the following results:

1. The maximum weight loss rate, or mean depth of penetration rate (MDPR), in mineral oil D21 was four times that in water. However, the MDPR decreased continuously with further test time in mineral oil.

2. The cavitation erosion pits were of smaller diameter

in mineral oil D21 than the pits in water for the same depth. The pits in general have a deeper central portion with shallow flat portions on either side.

3. The ratio of pit depth to pit radius at the surface  $h/a$  of individual pits varied from 0.125 to 0.400 in mineral oil and from 0.075 to 0.260 in water. Considering pits of depth less than  $15 \mu\text{m}$  only, we found that in mineral oil  $h/a = 0.312$  and in water  $h/a = 0.220$ .

Lewis Research Center  
National Aeronautics and Space Administration  
Cleveland, Ohio, March 18, 1983

## References

- Garner, D. R.; James, R. D.; and Warriner, J. F.: Cavitation Erosion Damage in Engine Bearings: Theory and Practice. *J. Eng. Power*, vol. 102, no. 4, Oct. 1980, pp. 847-857.
- Wilson, R. W.: Cavitation Damage in Plain Bearings. Cavitation and Related Phenomena in Lubrication. D. Dowson, M. Godet, and C. M. Taylor, eds., Institution of Mechanical Engineers (London), 1975, pp. 177-184.
- Summers-Smith, D.: Discussion on Cavitation Damage. Cavitation and Related Phenomena. D. Dowson, M. Godet, and C. M. Taylor, eds., Institution of Mechanical Engineers (London), 1975, pp. 198-199.
- Conway-Jones, J. M.: Discussion on Cavitation Damage. Cavitation and Related Phenomena. D. Dowson, M. Godet and C. M. Taylor, eds., Institution of Mechanical Engineers (London), 1975, pp. 201-217.
- James, R. D.: Erosion Damage in Engine Bearings. *Tribol. Int.*, vol. 8, no. 4, 1975, pp. 161-170.
- Dowson, D.; and Taylor, C. M.: Cavitation in Bearings. *Annual Review of Fluid Mechanics*. Vol. 11. M. Van Dyke, J. V. Wehausen, and J. L. Lumley, eds., Annual Reviews, Inc., 1979, pp. 35-66.
- Hunt, J. B.; Ryde-Weller, A. J.; and Ashmead, F. A. H.: Cavitation Between Meshing Gear Teeth. *Wear*, vol. 71, 1981, pp. 65-78.
- Heathcock, C. J.; and Protheroe, B. E.: Cavitation Erosion of Stainless Steels. *Wear*, vol. 81, 1982, pp. 311-327.
- Endo, K.; Okada, T.; and Nakashima, M.: A Study of Erosion Between Two Parallel Surfaces Oscillating at Close Proximity in Liquids. *J. Lubr. Technol.*, vol. 89, no. 3, July 1967, pp. 229-236.
- Soda, N.; and Tanaka, Y.: Cavitation Erosion of Flat Surface Near Rotating Shaft. *Wear of Materials 1981*. S. K. Rhee, A. W. Ruff, and K. C. Ludema, eds., ASME, 1981, pp. 607-612.
- Vyas, B.; and Preece, C. M.: Stress Produced in a Solid by Cavitation. *J. Appl. Phys.*, vol. 47, no. 12, Dec. 1976, pp. 5133-5138.
- Ivany, R. D.; and Hammitt, F. G.: Cavitation Bubble Collapse in Viscous Compressible Liquids—Numerical Analysis. *J. Basic Eng.*, vol. 87, no. 4, Dec. 1965, pp. 977-985.
- Plesset, M. S.: Bubble Dynamics. *Cavitation in Real Liquids*. Robert Davies, ed., Elsevier Publishing Company, 1964, pp. 1-18.
- Robinson, M. J.; and Hammitt, F. G.: Detailed Damage Characteristics in a Cavitating Venturi. *J. Basic Eng.*, vol. 89, no. 1, Mar. 1967, pp. 161-173.
- Stinebring, D. R.; Holl, J. W.; and Arndt, R. E. A.: Two Aspects of Cavitation Damage in the Incubation Zone—Scaling by Energy Considerations and Leading Edge Damage. *J. Fluids Eng.*, vol. 102, no. 4, Dec. 1980, pp. 481-485.



1. Report No. NASA TP-2146		2. Government Accession No.		3. Recipient's Catalog No.	
4. Title and Subtitle CAVITATION PITTING AND EROSION OF ALUMINUM 6061-T6 IN MINERAL OIL AND WATER				5. Report Date August 1983	
7. Author(s) Bezzam C. S. Rao and Donald H. Buckley				6. Performing Organization Code 506-53-1B	
9. Performing Organization Name and Address National Aeronautics and Space Administration Lewis Research Center Cleveland, Ohio 44135				8. Performing Organization Report No. E-1516	
12. Sponsoring Agency Name and Address National Aeronautics and Space Administration Washington, D. C. 20546				10. Work Unit No.	
15. Supplementary Notes Bezzam C. S. Rao, Indian Institute of Science, Bangalore, India, and National Research Council - NASA Research Associate; Donald H. Buckley, Lewis Research Center. Presented in part at ASME Cavitation and Polyphase Flow Forum, Houston, Texas, June 20-22, 1983.				11. Contract or Grant No.	
16. Abstract Cavitation erosion studies of aluminum 6061-T6 in mineral oil and in ordinary tap water are presented. The maximum erosion rate (MDPR, or mean depth of penetration rate) in mineral oil was about four times that in water. The MDPR in mineral oil decreased continuously with time, but the MDPR in water remained approximately constant. The cavitation pits in mineral oil were of smaller diameter and depth than the pits in water. Treating the pits as spherical segments, we computed the radius $r$ of the sphere. The logarithm of $h/a$ , where $h$ is the pit depth and $2a$ is the top width of the pit, was linear when plotted against the logarithm of $2r/h - 1$ .				13. Type of Report and Period Covered Technical Paper	
17. Key Words (Suggested by Author(s)) Cavitation erosion      Aluminum Mineral oil              Pitting Water                      Lubrication				14. Sponsoring Agency Code	
18. Distribution Statement Unclassified - unlimited STAR Category 37					
19. Security Classif. (of this report) Unclassified		20. Security Classif. (of this page) Unclassified		21. No. of Pages 8	
				22. Price* A01	

National Aeronautics and  
Space Administration

Washington, D.C.  
20546

Official Business

Penalty for Private Use, \$300

THIRD-CLASS BULK RATE

Postage and Fees Paid  
National Aeronautics and  
Space Administration  
NASA-451



2 1 1U,D, 830810 S00903DS  
DEPT OF THE AIR FORCE  
AF WEAPONS LABORATORY  
ATTN: TECHNICAL LIBRARY (SUL)  
KIRTLAND AFB NM 87117

**NASA**

Table (Section 158  
ual) Do Not Return